

# On the Adsorption of Atomic Arsenic and Arsenous Acid on the Graphene-Oxide: A DFT Study

Art Anthony Z. Munio<sup>1,2</sup> , Alvanh Alem G. Pido<sup>3</sup> , Diamond C. Domato<sup>2,4</sup> , Leo Cristobal C. Ambolode II<sup>2,4</sup> 

<sup>1</sup> College of Arts and Sciences, Jose Rizal Memorial State University, 7120 Dapitan, Zamboanga del Norte, Philippines

<sup>2</sup> Physics Department, Mindanao State University – Iligan Institute of Technology, 9200 Iligan City, Philippines

<sup>3</sup> Department of Physics, Mindanao State University-Main Campus, 9700 Marawi City, Philippines

<sup>4</sup> Premier Research Institute of Science and Mathematics (PRISM), Mindanao State University – Iligan Institute of Technology, 9200 Iligan City, Philippines

\* Correspondence: [artanthony.munio@g.msuit.edu.ph](mailto:artanthony.munio@g.msuit.edu.ph);

Received: 23.05.2023; Accepted: 11.08.2023; Published: 5.09.2025

**Abstract:** The detrimental effect of Arsenic (As) on the water system is a primary concern worldwide. This study assessed the adsorption capabilities of graphene oxide as an adsorbent material for Arsenic (As) using first-principles density functional theory. Results indicate that the atomic As can strongly interact with the carbon atoms of graphene oxide. However, the results also suggest that As appears to form an As-O species when it comes into contact with the oxygen functional groups of the graphene oxide. Meanwhile, the adsorption of As(III) in the form of As(OH)<sub>3</sub> on the graphene oxide is described mainly by physisorption. These claims are obtained by evaluating the strength of interaction, electron redistribution, and density of states of the studied configurations. This work provides a fundamental understanding of the interaction of graphene-oxide with atomic As and As(III).

**Keywords:** arsenic; As(OH)<sub>3</sub>; adsorption; density functional theory; graphene oxide.

© 2025 by the authors. This article is an open-access article distributed under the terms and conditions of the Creative Commons Attribution (CC BY) license (<https://creativecommons.org/licenses/by/4.0/>), which permits unrestricted use, distribution, and reproduction in any medium, provided the original work is properly cited. The authors retain copyright of their work, and no permission is required from the authors or the publisher to reuse or distribute this article, as long as proper attribution is given to the original source.

## 1. Introduction

The growing levels of global industrialization unintentionally introduce harmful inorganic compounds into the environment [1–3]. The environment is regularly adversely affected, which can have catastrophic effects on freshwater resources and aquatic life [4,5]. One of the most prominent water pollutants is Arsenic (As), mainly from manufacturing facilities, electronic waste, and agricultural waste discharged into water systems [6,7]. The detrimental effects of severe As on human health have been connected to various malignancies, immune system issues, cognitive impairments, and other conditions [8,9]. Additionally, as a significant factor in As contamination, some areas of the world have higher quantities of As deposits in the soil and groundwater [10,11]. Therefore, removing these inorganic chemicals is crucial in securing aquatic life and avoiding human intake. For this reason, various adsorbent materials, such as metal oxides, biopolymers, and graphene-based nanomaterials, are explored [12–17].

Graphene-based nanomaterials are attractive for heavy metal adsorption due to their large surface area and can be used as a template for adding nanomaterials for nano-engineering

the interaction of water pollutants [18–20]. The high surface area (2600 m<sup>2</sup>/g), impressive mechanical properties, and tunable chemical reactivities make it an ideal material for efficient adsorbent material [21]. Graphene is a two-dimensional material composed of carbon atoms bonded in *sp*<sup>2</sup> hybridization. This nanomaterial has become a subject of interest for decades due to its unique properties, becoming the most studied material. However, due to the strong van der Waals interaction between the layers, graphene layers typically form a stacked structure, also known as graphite. The properties above are not demonstrated in their stacked form. The isolation of graphene in solution is difficult owing to its inert surface. This problem has hindered practical applications of graphene and other carbon-based nanomaterials until now. The usual treatment of the graphene dispersion problem is by covalent functionalization of oxygen functional groups [22]. This modified graphene is known as graphene-oxide and reduced graphene-oxide, depending on the level of oxygen functional groups. The dominant functional groups of graphene-oxide are epoxide (-O) and hydroxyl (-OH) groups [23].

Various scientific reports already show that graphene-based materials and their composites are practical and efficient as an adsorbent material for various water pollutants, particularly heavy ones, as discussed in the following references [24–27]. However, limited efforts are conducted to analyze the interaction of these heavy metals with graphene-based materials. An in-depth understanding of the adsorption mechanism is a prerequisite for developing efficient adsorbent materials to remove heavy metals from water. The typical methodology to accurately study chemical interaction is to use a simulation method based on principles of quantum mechanics [28–31]. Quantum-based simulation methodology eliminates trial and error in experimental work and helps explain its findings.

This study uses density functional theory to assess the adsorption of atomic As and As(III) (in the form of As(OH)<sub>3</sub>) on the graphene oxide. In both cases, As and As(OH)<sub>3</sub> spontaneously adsorbed on the graphene-oxide, indicated by a negative value of the binding energy. The interaction of As(OH)<sub>3</sub> with the graphene oxide is mainly characterized by physisorption. Hydrogen bonding is formed between As(OH)<sub>3</sub> and the functional groups of graphene oxide. On the other hand, the atomic As is chemically adsorbed on the graphene oxide. However, when the atomic As interacts with the oxygen functional groups of the graphene oxide, an As-O species is formed. These findings provide a fundamental understanding and new insights into the adsorption mechanism of atomic As and As(OH)<sub>3</sub> on graphene oxide.

## 2. Materials and Methods

All DFT calculations are performed using Quantum Espresso with optimized norm-conserving pseudopotentials, PBE exchange-correlation functional, plane-wave bases set, and Grimme-D3 to consider the long-range interactions [32–36]. The cutoff energy and charge are set to their standard value, 60 Ry and 240 Ry, respectively. The *scf* energy convergence criteria are set to 10<sup>-8</sup> Ry. The force threshold is set to 10<sup>-4</sup> Ry/Bohr per atom during the optimization of the atomic configurations. The  $\Gamma$ -point algorithm is utilized for all calculations to estimate the ground-state atomic configuration. A  $5 \times 5 \times 1$  k-point sampling is utilized to obtain the binding energy. A 15 Å vacuum is included to remove the interaction of adjacent images. The charge density difference and electron localization function are calculated for all optimized structures to study the electron redistribution due to the adsorption further. The charge transfer is calculated using the Bader Charge Analysis using the code developed by Henkelman [37–

40]. Lastly, the total and local density of states are calculated using the tetrahedra method, considering  $8 \times 8 \times 1$  k-points sampling.

### 3. Results and Discussion

The model of the graphene oxide is shown in Figure 1a and Figure 1b. In the graphene-oxide system, a single epoxide and hydroxy group are adsorbed on graphene. The  $l_1$ ,  $l_2$ , and  $l_3$  C-O bonds of the epoxide and hydroxyl group are 1.49 Å, 1.44 Å, and 1.47 Å, respectively. The hydrogen bond between epoxide and hydroxyl is 1.95 Å. Now in the  $\text{As}(\text{OH})_3$ , the  $T_1$ ,  $T_2$ , and  $T_3$  As-O bond is 1.80 Å, 1.80 Å, and 1.83 Å, respectively. The measured bond lengths of graphene-oxide and  $\text{As}(\text{OH})_3$  presented here agree with existing reports [23,41,42].

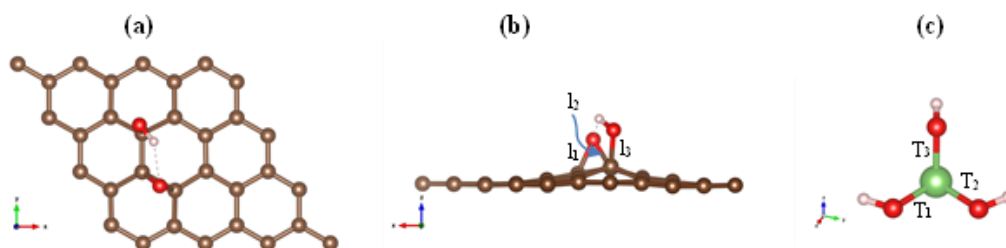


**Figure 1.** The optimized atomic configuration of a  $4 \times 4 \times 1$  supercell of graphene with adsorbed epoxide and hydroxyl group viewed from (a) top; (b) side. (c) The optimized configuration of isolated  $\text{As}(\text{OH})_3$ .

The optimized As configuration on the graphene oxide is displayed in Figure 2. The binding energy of Figure 2a is -1.59 eV. In Figure 2b, the As interaction is initially placed at the top of the epoxide and hydroxyl. After full optimization, the As-O formed species detaches the graphene-oxide functional groups. The measured graphene-As equilibrium distance of Figure 2b is 3.32 Å. The results obtained here were also observed by Panigrahi et al. [42]. On the other hand, in Figure 3a and Figure 3b, the binding energy of the  $\text{As}(\text{OH})_3$  on the graphene-oxide is -0.33 eV and -0.36 eV, respectively. The binding energy in Figure 3b is relatively stronger due to the hydrogen bonding between the hydroxyl and  $\text{As}(\text{OH})_3$ . The equilibrium distances of As with the graphene-oxide in Figure 3a and Figure 3b are 3.54 Å and 3.16 Å, respectively. Based on the equilibrium distance and strength of interaction, one can point out that the As can be chemically adsorbed on the carbon atoms of graphene oxide. While  $\text{As}(\text{OH})_3$  is adsorbed via physisorption mainly due to van der Waals and hydrogen bonding.

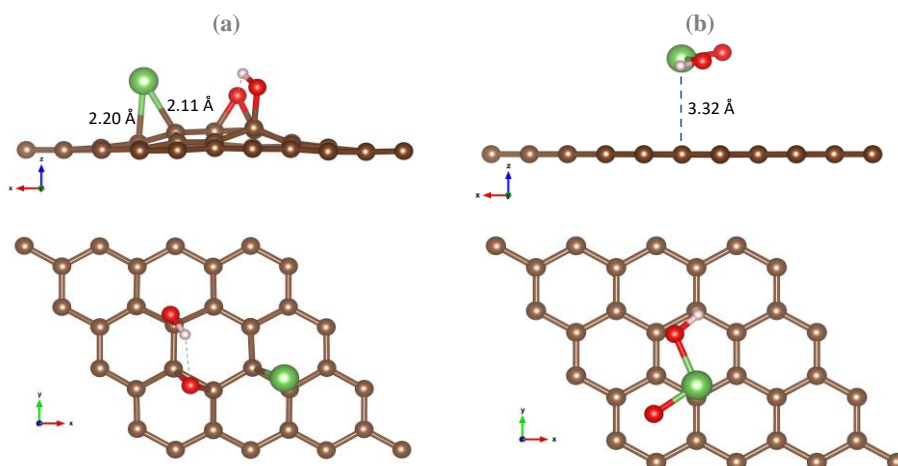


**Figure 2.** The optimized configuration of As on the surface of graphene oxide at two distinct initial conditions.

(a) The initial placement of As is adsorbed on the C-C bond of graphene oxide and distant from its oxygen functional groups; (b) The initial configuration of As is on top of the oxygen functional groups of the graphene oxide.

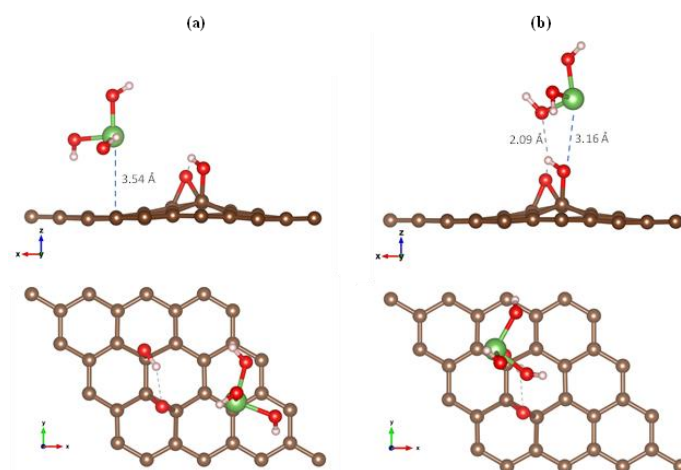


**Figure 3.** The optimized configuration of graphene-oxide with adsorbed  $\text{As(OH)}_3$ . The initial placement of  $\text{As(OH)}_3$  is (a) distant from the oxygen functional groups; (b) above the oxygen functional groups.

The charge redistributions of the optimized structures represented by the Charge Density Difference are shown in Figure 4a- Figure 4c. It is evident in Figure 4a that the depletion of the electronic charge is mainly in the C atoms of the graphene oxide in the vicinity of adsorbed As. It is also observable that the accumulation of the electronic charge is present in the C-As bond, indicating a strong interaction of the C atoms and As. This result further verifies the calculated binding energy. The Bader charge transfer in Figure 3a yields 0.27 e, and the electrons accumulate towards the adsorbed As. In the  $\text{As(OH)}_3$  and graphene-oxide system in Figure 4b, the charge redistribution is dominantly observed in the interface of graphene-oxide and  $\text{As(OH)}_3$ , with minimal charge redistribution visible on the functional groups. In Figure 4c, the functional groups of the graphene oxide play an essential role in establishing a hydrogen bond between the hydroxyl group and the  $\text{As(OH)}_3$ . These configurations yield a negligible charge transfer, justifying their weak synergetic interaction, a common feature of physisorption.

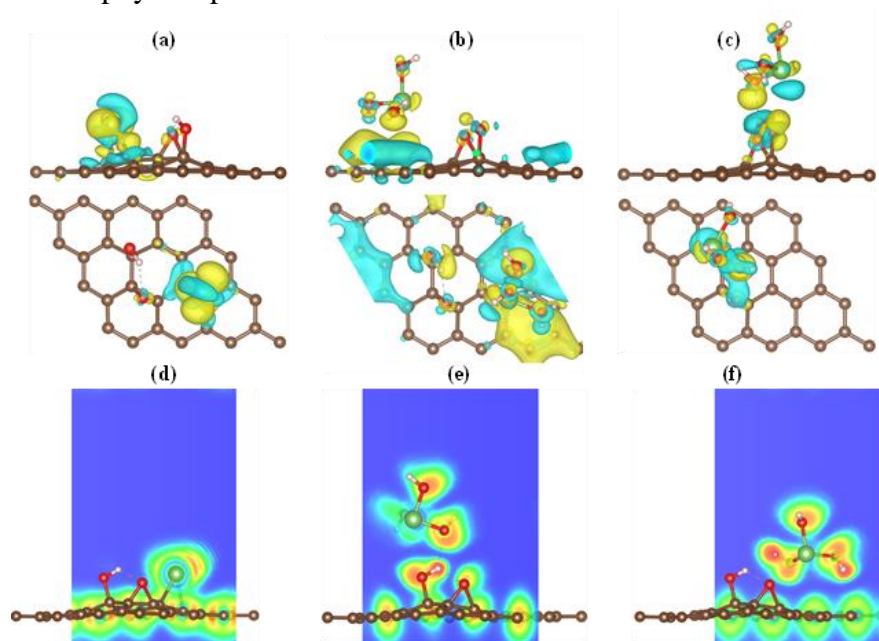


**Figure 4.** The electronic redistributions of the As and  $\text{As(OH)}_3$  adsorption on the graphene-oxide are represented by charge density difference and electron localization function. (a)-(c) isosurface of charge density difference; (d)-(f) 2D electron localization function of the studied configurations.

To further understand the electronic redistribution, the 2D Electron Localization Functions (ELF) of the studied configurations are calculated and displayed in Figure 4c and Figure 4d. Green ELF basins are observed at the interface of adsorbed As and graphene oxide, indicating a sharing of electrons (Figure 4d). Meanwhile, a deep blue region is kept at the interface of the graphene oxide and As(OH)<sub>3</sub>, as displayed in Figure 4e and Figure 4f, indicating the physisorption type of interaction. This claim is supported and reflected in the strength of interaction, charge transfer, and equilibrium distances, as summarized in Table 1.

**Table 1.** Summary of the bonding type, interaction distance, binding energy, charge transfer, and bandgap of the studied configurations.

System	Bonding type	Interaction distance (Å)	Binding energy (eV)	Charge transfer (e)	Bandgap (eV)
Fig.2a. GO-As	Chemical	2.11	-1.51	$2.7 \times 10^{-1}$	0.26 eV
Fig.3a. GO-As(OH) <sub>3</sub>	Physical	3.54	-0.27	$2.0 \times 10^{-2}$	0 eV
Fig.3b GO-As(OH) <sub>3</sub>	Physical	2.09	-0.35	$6.6 \times 10^{-4}$	0 eV

\*Accumulation of electrons into the As and As(OH)<sub>3</sub>.

The plots of the density of states of the studied configurations are displayed in Figure 5. The graphene oxide of our model shows a metallic nature, indicated by states appearing at the Fermi level (see Figure 5a). The adsorption of As on the graphene oxide significantly modified the density of states. Particularly in the vicinity of the Fermi level, which opens the bandgap of 0.26 eV (Figure 5b). Further calculations on the local density of states LDOS are displayed in Figure 6, indicating strong orbital hybridization of the 2*p* orbital characters of the two nearest C atoms (C<sub>1</sub> and C<sub>2</sub>) with the 4*p* orbital of As. This further supports the chemical interaction of the As with the graphene oxide. On the other hand, the density of states of the graphene-oxide and As(OH)<sub>3</sub> shows no significant hybridization of the orbitals. This is evident in the density of states of the graphene-oxide, which is well maintained in Figures 5c and 5d.

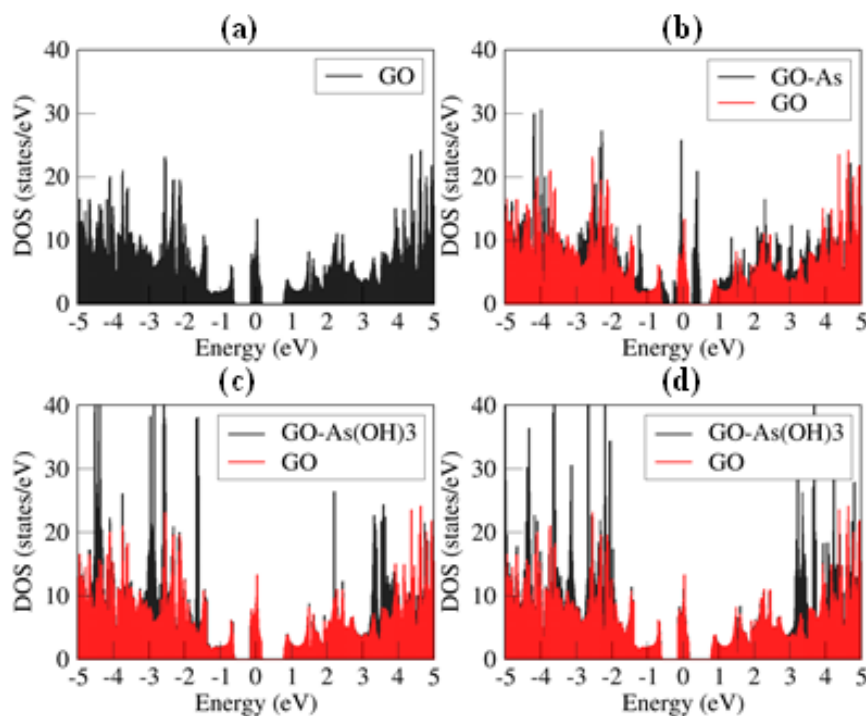


**Figure 5.** The electronic density of states of the studied configurations: (a) graphene-oxide; (b) graphene-oxide with adsorbed As (Figure 2a), graphene-oxide with adsorbed As(OH)<sub>3</sub> shown in (c) Figure 3a; (d) Figure 3b.

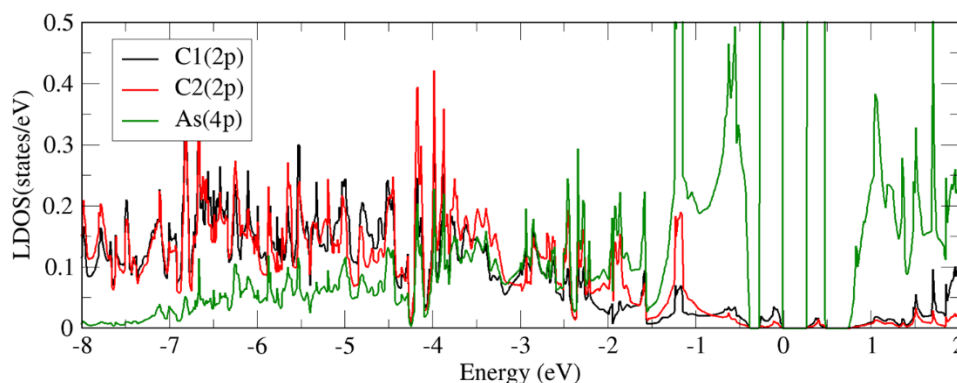


**Figure 6.** The local density of states hybridization of As(4p) and C(2p) of the atomic As and graphene-oxide, respectively.

#### 4. Conclusions

First-principles density functional theory calculations were conducted to investigate the interaction of graphene-oxide with the atomic As and As(OH)<sub>3</sub>. The results indicate that the As can interact chemically with the neighboring C atoms of the graphene oxide. However, if the As is placed near the epoxide and hydroxyl group, this will detach the functional groups to form the As-O species. On the other hand, the interaction of As(OH)<sub>3</sub> with the graphene oxide is mainly described as physisorption. This conclusion is drawn based on the strength of interaction, charge density difference, ELF, Bader charge transfer analysis, and electronic density of states. This work clarifies previous experimental efforts on related systems and will serve as a reference for future work on graphene-based materials for removing toxic heavy metals from water sources.

#### Author Contributions

All authors have read and agreed to the published version of the manuscript.

#### Institutional Review Board Statement

Not applicable.

#### Informed Consent Statement

Not applicable.

#### Data Availability Statement

Data supporting the findings of this study are available upon reasonable request from the corresponding author.

#### Funding

A.A.Z.M. received funding from the Higher Education Research and Innovation Fund through the project titled “In Search for the Next-Generation of Adsorbent and Sensing Material for Heavy Metals via Quantum Chemical Calculations Using Super-Computing Platform,” implemented at Jose Rizal Memorial State University – Tampilisan Campus.

## Acknowledgments

A.A.Z.M. acknowledges the auspicious support of the College of Arts and Sciences, Research Unit, and Administration of Jose Rizal Memorial State University – Tampilisan Campus. A.A.Z.M., A.A.G.P., D.C.D., and L.C.C.A.II also received assistance from Mindanao State University – Iligan Institute of Technology and Mindanao State University – Main Campus by partly providing the computational resources.

## Conflicts of Interest

The authors declare no conflict of interest.

## References

1. Saravanan, A.; Kumar, P.S.; Hemavathy, R.V.; Jeevanantham, S.; Harikumar, P.; Priyanka, G.; Devakirubai, D.R.A. A comprehensive review on sources, analysis and toxicity of environmental pollutants and its removal methods from water environment. *Sci. Total Environ.* **2022**, *812*, 152456, <http://doi.org/10.1016/j.scitotenv.2021.152456>.
2. Miranda, L.S.; Ayoko, G.A.; Egodawatta, P.; Goonetilleke, A. Adsorption- desorption behavior of heavy metals in aquatic environments: Influence of sediment, water and metal ionic properties. *J. Hazard. Mater.* **2022**, *421*, 126743, <http://doi.org/10.1016/j.jhazmat.2021.126743>.
3. Zamora-Ledezma, C.; Negrete-Bolagay, D.; Figueroa, F.; Zamora-Ledezma, E.; Ni, M.; Alexis, F.; Guerrero, V.H. Heavy metal water pollution: A fresh look about hazards, novel and conventional remediation methods. *Environ. Technol. Innov.* **2021**, *22*, 101504, <http://doi.org/10.1016/j.eti.2021.101504>.
4. Lin, L.; Yang, H.; Xu, X. Effects of Water Pollution on Human Health and Disease Heterogeneity: A Review. *Front. Environ. Sci.* **2022**, *10*, 880246, <https://doi.org/10.3389/fenvs.2022.880246>.
5. Paronda, G.R.A.; David, C.P.C.; Apodaca, D.C. River flow pattern and heavy metals concentrations in Pasig River, Philippines as affected by varying seasons and astronomical tides. *IOP Conf. Ser.: Earth Environ. Sci.* **2019**, *344*, 012049, <http://doi.org/10.1088/1755-1315/344/1/012049>.
6. Garelick, H.; Jones, H.; Dybowska, A.; Valsami-Jones, E. Arsenic Pollution Sources. In *Reviews of Environmental Contamination and Toxicology*, Springer, New York, NY, **2008**, Volume 197, 17–60, [http://doi.org/10.1007/978-0-387-79284-2\\_2](http://doi.org/10.1007/978-0-387-79284-2_2).
7. López, J.; Reig, M.; Vecino, X.; Cortina, J.L. Arsenic impact on the valorisation schemes of acidic mine waters of the Iberian Pyrite Belt: Integration of selective precipitation and spiral-wound nanofiltration processes. *J. Hazard. Mater.* **2021**, *403*, 123886, <http://doi.org/10.1016/j.jhazmat.2020.123886>.
8. Singh, R.; Singh, S.; Parihar, P.; Singh, V.P.; Prasad, S.M. Arsenic contamination, consequences and remediation techniques: A review. *Ecotoxicol. Environ. Saf.* **2015**, *112*, 247–270, <http://doi.org/10.1016/j.ecoenv.2014.10.009>.
9. Ozturk, M.; Metin, M.; Altay, V.; Bhat, R.A.; Ejaz, M.; Gul, A.; Unal, B.T.; Hasanuzzaman, M.; Nibir, L.; Nahar, K.; Bukhari, A.; Dervash, M.A.; Kawano, T. Arsenic and Human Health: Genotoxicity, Epigenomic Effects, and Cancer Signaling. *Biol. Trace Elem. Res.* **2022**, *200*, 988–1001, <http://doi.org/10.1007/s12011-021-02719-w>.
10. Shankar, S.; Shanker, U.; Shikha. Arsenic Contamination of Groundwater: A Review of Sources, Prevalence, Health Risks, and Strategies for Mitigation. *Sci. World J.* **2014**, *2014*, 304524, <http://doi.org/10.1155/2014/304524>.
11. Monteiro De Oliveira, E.C.; Caixeta, E.S.; Santos, V.S.V.; Pereira, B.B. Arsenic exposure from groundwater: environmental contamination, human health effects, and sustainable solutions. *J. Toxicol. Environ. Health B Crit Rev.* **2021**, *24*, 119–135, <http://doi.org/10.1080/10937404.2021.1898504>.
12. Mosafieri, M.; Nemati, S.; Khataee, A.; Nasser, S.; Hashemi, A.A. Removal of Arsenic (III, V) from aqueous solution by nanoscale zero-valent iron stabilized with starch and carboxymethyl cellulose. *J. Environ. Health Sci. Eng.* **2014**, *12*, 74, <http://doi.org/10.1186/2052-336X-12-74>.
13. Shakoor, M.B.; Ali, S.; Rizwan, M.; Abbas, F.; Bibi, I.; Riaz, M.; Khalil, U.; Niazi, N.K.; Rinklebe, J. A review of biochar-based sorbents for separation of heavy metals from water. *Int. J. Phytoremediation* **2020**, *22*, 111–126, <http://doi.org/10.1080/15226514.2019.1647405>.

14. Kaur, J.; Sengupta, P.; Mukhopadhyay, S. Critical Review of Bioadsorption on Modified Cellulose and Removal of Divalent Heavy Metals (Cd, Pb, and Cu). *Ind. Eng. Chem. Res.* **2022**, *61*, 1921–1954, <http://doi.org/10.1021/acs.iecr.1c04583>.
15. Najib, N.; Christodoulatos, C. Removal of arsenic using functionalized cellulose nanofibrils from aqueous solutions. *J. Hazard. Mater.* **2019**, *367*, 256–266, <http://doi.org/10.1016/j.jhazmat.2018.12.067>.
16. Syeda, H.I.; Yap, P.-S. A Review on three-dimensional cellulose-based aerogels for the removal of heavy metals from water. *Sci. Total Environ.* **2022**, *807*, 150606, <http://doi.org/10.1016/j.scitotenv.2021.150606>.
17. Pradhan, S.S.; Konwar, K.; Ghosh, T.N.; Mondal, B.; Sarkar, S.K.; Deb, P. Multifunctional Iron oxide embedded reduced graphene oxide as a versatile adsorbent candidate for effectual arsenic and dye removal. *Colloid Interface Sci. Commun.* **2020**, *39*, 100319, <http://doi.org/10.1016/j.colcom.2020.100319>.
18. Xu, J.; Cao, Z.; Zhang, Y.; Yuan, Z.; Lou, Z.; Xu, X.; Wang, X. A review of functionalized carbon nanotubes and graphene for heavy metal adsorption from water: Preparation, application, and mechanism. *Chemosphere* **2018**, *195*, 351–364, <http://doi.org/10.1016/j.chemosphere.2017.12.061>.
19. Peng, W.; Li, H.; Liu, Y.; Song, S. A review on heavy metal ions adsorption from water by graphene oxide and its composites. *J. Mol. Liq.* **2017**, *230*, 496–504, <http://doi.org/10.1016/j.molliq.2017.01.064>.
20. Adel, M.; Ahmed, M.A.; Elabiad, M.A.; Mohamed, A.A. Removal of heavy metals and dyes from wastewater using graphene oxide-based nanomaterials: A critical review. *Environ. Nanotechnol. Monit. Manag.* **2022**, *18*, 100719, <http://doi.org/10.1016/j.enmm.2022.100719>.
21. Allen, M.J.; Tung, V.C.; Kaner, R.B. Honeycomb Carbon: A Review of Graphene. *Chem. Rev.* **2010**, *110*, 132–145, <http://doi.org/10.1021/cr900070d>.
22. Georgakilas, V.; Otyepka, M.; Bourlinos, A.B.; Chandra, V.; Kim, N.; Kemp, K.C.; Hobza, P.; Zboril, R.; Kim, K.S. Functionalization of Graphene: Covalent and Non-Covalent Approaches, Derivatives and Applications. *Chem. Rev.* **2012**, *112*, 6156–6214, <http://doi.org/10.1021/cr3000412>.
23. Luo, H.; Auchterlonie, G.; Zou, J. A thermodynamic structural model of graphene oxide. *J. Appl. Phys.* **2017**, *122*, 145101, <http://doi.org/10.1063/1.4991967>.
24. Du, B.; Chai, L.; Li, W.; Wang, X.; Chen, X.; Zhou, J.; Sun, R.-C. Preparation of functionalized magnetic graphene oxide/lignin composite nanoparticles for adsorption of heavy metal ions and reuse as electromagnetic wave absorbers. *Sep. Purif. Technol.* **2022**, *297*, 121509, <http://doi.org/10.1016/j.seppur.2022.121509>.
25. Ibrahim, Y.; Wadi, V.S.; Ouda, M.; Naddeo, V.; Banat, F.; Hasan, S.W. Highly selective heavy metal ions membranes combining sulfonated polyethersulfone and self-assembled manganese oxide nanosheets on positively functionalized graphene oxide nanosheets. *Chem. Eng. J.* **2022**, *428*, 131267, <http://doi.org/10.1016/j.cej.2021.131267>.
26. Vasseghian, Y.; Dragoi, E.-N.; Almomani, F.; Le, V.T.; Berkani, M. Graphene- based membrane techniques for heavy metal removal: A critical review. *Environ. Technol. Innov.* **2021**, *24*, 101863, <http://doi.org/10.1016/j.eti.2021.101863>.
27. Khan, Z.U.; Khan, W.U.; Ullah, B.; Ali, W.; Ahmad, B.; Ali, W.; Yap, P.-S. Graphene oxide/PVC composite papers functionalized with p-Phenylenediamine as high-performance sorbent for the removal of heavy metal ions. *J. Environ. Chem. Eng.* **2021**, *9*, 105916, <http://doi.org/10.1016/j.jece.2021.105916>.
28. Burke, K. Perspective on density functional theory. *J. Chem. Phys.* **2012**, *136*, 150901, <http://doi.org/10.1063/1.4704546>.
29. Chakraborty, D.; Chattaraj, P.K. Conceptual density functional theory based electronic structure principles. *Chem. Sci.* **2021**, *12*, 6264–6279, <http://doi.org/10.1039/D0SC07017C>.
30. Liao, X.; Lu, R.; Xia, L.; Liu, Q.; Wang, H.; Zhao, K.; Wang, Z.; Zhao, Y. Density Functional Theory for Electrocatalysis. *Energy Environ. Mater.* **2022**, *5*, 157–185, <http://doi.org/10.1002/eam2.12204>.
31. Kushwaha, A.K. A Brief Review of Density Functional Theory and Solvation Model. ChemRxiv, Cambridge, **2022**, <http://doi.org/10.26434/chemrxiv-2022-vlhm0>.
32. Giannozzi, P.; Baroni, S.; Bonini, N.; Calandra, M.; Car, R.; Cavazzoni, C.; Ceresoli, D.; Chiarotti, G.L.; Cococcioni, M.; Dabo, I.; Dal Corso, A.; de Gironcoli, S.; Fabris, S.; Fratesi, G.; Gebauer, R.; Gerstmann, U.; Gougousis, C.; Kokalj, A.; Lazzeri, M.; Martin-Samos, L.; Marzari, N.; Mauri, F.; Mazzarello, R.; Paolini, S.; Pasquarello, A.; Paulatto, L.; Sbraccia, C.; Scandolo, S.; Sclauzero, G.; Seitsonen, A.P.; Smogunov, A.; Umari, P.; Wentzcovitch, R.M. QUANTUM ESPRESSO: a modular and open-source software project for quantum simulations of materials. *J. Phys. Condens. Matter.* **2009**, *21*, 395502, <http://doi.org/10.1088/0953-8984/21/39/395502>.

33. Giannozzi, P.; Barone, O.; Bonfà, P.; Brunato, D.; Car, R.; Carnimeo, I.; Cavazzoni, C.; de Gironcoli, S.; Delugas, P.; Ferrari Ruffino, F.; Ferretti, A.; Marzari, N.; Timrov, I.; Urru, A.; Baroni, S. Quantum ESPRESSO toward the exascale. *J. Chem. Phys.* **2020**, *152*, 154105, <http://doi.org/10.1063/5.0005082>.
34. Hamann, D.R. Optimized norm-conserving Vanderbilt pseudopotentials. *Phys. Rev. B* **2013**, *88*, 085117, <http://doi.org/10.1103/PhysRevB.88.085117>.
35. Perdew, J.P.; Burke, K.; Ernzerhof, M. Generalized Gradient Approximation Made Simple. *Phys. Rev. Lett.* **1996**, *77*, 3865, <http://doi.org/10.1103/PhysRevLett.77.3865>.
36. Grimme, S.; Antony, J.; Ehrlich, S.; Krieg, H. A consistent and accurate *ab initio* parametrization of density functional dispersion correction (DFT-D) for the 94 elements H-Pu. *J. Chem. Phys.* **2010**, *132*, 154104, <http://doi.org/10.1063/1.3382344>.
37. Tang, W.; Sanville, E.; Henkelman, G. A grid-based Bader analysis algorithm without lattice bias. *J. Phys.: Condens. Matter* **2009**, *21*, 084204, <http://doi.org/10.1088/0953-8984/21/8/084204>.
38. Sanville, E.; Kenny, S.D.; Smith, R.; Henkelman, G. Improved grid-based algorithm for Bader charge allocation. *J. Comput. Chem.* **2007**, *28*, 899–908, <http://doi.org/10.1002/jcc.20575>.
39. Henkelman, G.; Arnaldsson, A.; Jónsson, H. A fast and robust algorithm for Bader decomposition of charge density. *Comput. Mater. Sci.* **2006**, *36*, 354–360, <http://doi.org/10.1016/j.commatsci.2005.04.010>.
40. Yu, M.; Trinkle, D.R. Accurate and efficient algorithm for Bader charge integration. *J. Chem. Phys.* **2011**, *134*, 064111, <http://doi.org/10.1063/1.3553716>.
41. Dzade, N.Y.; Roldan, A.; de Leeuw, N.H. Structures and Properties of As(OH)<sub>3</sub> Adsorption Complexes on Hydrated Mackinawite (FeS) Surfaces: A DFT-D2 Study. *Environ. Sci. Technol.* **2017**, *51*, 3461–3470, <http://doi.org/10.1021/acs.est.7b00107>.
42. Panigrahi, P.; Dhinakaran, A.K.; Sekar, Y.; Ahuja, R.; Hussain, T. Efficient Adsorption Characteristics of Pristine and Silver-Doped Graphene Oxide Towards Contaminants: A Potential Membrane Material for Water Purification? *ChemPhysChem* **2018**, *19*, 2250–2257, <http://doi.org/10.1002/cphc.201800223>.

## Publisher's Note & Disclaimer

The statements, opinions, and data presented in this publication are solely those of the individual author(s) and contributor(s) and do not necessarily reflect the views of the publisher and/or the editor(s). The publisher and/or the editor(s) disclaim any responsibility for the accuracy, completeness, or reliability of the content. Neither the publisher nor the editor(s) assume any legal liability for any errors, omissions, or consequences arising from the use of the information presented in this publication. Furthermore, the publisher and/or the editor(s) disclaim any liability for any injury, damage, or loss to persons or property that may result from the use of any ideas, methods, instructions, or products mentioned in the content. Readers are encouraged to independently verify any information before relying on it, and the publisher assumes no responsibility for any consequences arising from the use of materials contained in this publication.